

# 1 RETINOBLASTOMA RELATED (RBR) interaction with key factors of the RNA- 2 directed DNA methylation (RdDM) pathway.

3 León-Ruiz Jesús<sup>1+</sup>; Espinal-Centeno Annie<sup>1+</sup>; Blilou Ikram<sup>2</sup>; Scheres Ben<sup>3</sup>, Arteaga-Vázquez Mario<sup>4\*</sup>  
4 and Cruz-Ramírez Alfredo<sup>1\*</sup>.

- 5 1. Laboratory of Molecular and Developmental Complexity at Laboratorio Nacional de  
6 Genómica para la Biodiversidad, Centro de Investigación y de Estudios Avanzados del  
7 Instituto Politécnico Nacional, (CINVESTAV-IPN), 36590 Irapuato, México.
- 8 2. Biological and Environmental Science and Engineering Division (BESE), King Abdullah  
9 University of Science and Technology (KAUST), Thuwal, 23955 Saudi Arabia.
- 10 3. Laboratory of Molecular Biology, Department of Plant Sciences, Wageningen University,  
11 Wageningen, the Netherlands.
- 12 4. Group of Epigenetics and Developmental Biology, Instituto de Biotecnología y Ecología  
13 Aplicada (INBIOTECA), Universidad Veracruzana, 91090, Xalapa, México.

14  
15 + These authors contributed equally to this work

16 \*Authors for correspondence: [alfredo.cruz@cinvestav.mx](mailto:alfredo.cruz@cinvestav.mx), [maarteaga@uv.mx](mailto:maarteaga@uv.mx)

## 17 Summary

- 18 ● Transposable elements and other repetitive elements are silenced by the RNA-  
19 directed DNA methylation pathway (RdDM). In RdDM, POLIV-derived transcripts are  
20 converted into double stranded RNA (dsRNA) by the activity of RDR2 and  
21 subsequently processed into 24 nucleotide short interfering RNAs (24-nt siRNAs) by  
22 DCL3. 24-nt siRNAs are recruited by AGO4 and serve as guides to direct AGO4-  
23 siRNA complexes to chromatin bound POLV-derived transcripts generated from the  
24 template/target DNA. The interaction between POLV, AGO4, DMS3, DRD1, RDM1  
25 and DRM2 promotes DRM2-mediated *de novo* DNA methylation.
- 26 ● The Arabidopsis Retinoblastoma protein homolog is a master regulator of cell cycle,  
27 stem cell maintenance and development. *In silico* exploration of RBR protein  
28 partners revealed that several members of the RdDM pathway contain a motif that  
29 confers high affinity binding to RBR, including the largest subunits of POLIV and  
30 POLV (NRPD1 and NRPE1), the shared second largest subunit of POLIV and POLV  
31 (NRPD/E2), RDR1, RDR2, DCL3, DRM2 and SUVR2. We demonstrate that RBR  
32 binds to DRM2, DRD1 and SUVR2. We also report that seedlings from loss-of-  
33 function mutants in RdDM and in *RBR* show similar phenotypes in the root apical  
34 meristem. Furthermore, we show that RdDM and SUVR2 targets are up-regulated in  
35 the *35S::AmiGO-RBR* background.
- 36  
37 ● Our results suggest a novel mechanism for RBR function in transcriptional gene  
38 silencing based on the interaction with key players of the RdDM pathway and opens  
39 several new hypotheses, including the convergence of RBR-DRM2 on the  
40 transcriptional control of TEs and several cell/tissue and stage-specific target genes.

41 **Keywords:** RdDM, *de novo* DNA methylation, RETINOBLASTOMA, Development,  
42 epigenetics.

43

44

## 45 Introduction

46 DNA methylation is essential for proper development in eukaryotes. In plants,  
47 it is involved in the regulation of gene expression, the defense against invasive  
48 nucleic acids, both of them with effects on development and physiology. In plants,  
49 cytosines can be methylated in symmetrical (CG or CHG) and asymmetrical (CHH)  
50 sequence contexts (where H can be A, T, or C). Transposable elements (TEs) and  
51 other repetitive sequences are the main targets of DNA methylation (Borges and  
52 Martienssen, 2015; Matzke and Moshier, 2014). The major small RNA-mediated  
53 epigenetic pathway involved in *de novo* DNA methylation is the RNA-directed DNA  
54 methylation (RdDM) pathway (Matzke and Moshier, 2014; Erdmann and Picard,  
55 2020). RdDM involves the function of Nuclear RNA Polymerase D (NRPD) or POL  
56 IV and NRPE or POLV (Hagg and Pikaard, 2011). POLIV transcribes short single  
57 stranded RNA (ssRNA) 26 to 45 nt in length (from the target locus that will be  
58 methylated) that serve as substrate for RNA-DEPENDENT RNA POLYMERASE 2  
59 (RDR2) for the generation of double stranded RNA (dsRNA). The resulting dsRNA  
60 is processed by DICER-LIKE 3 (DCL3) into 24-nt small interfering RNAs (siRNAs).  
61 HUA ENHANCER 1 (HEN1) methylates 24-nt siRNAs at their 3'-end and are  
62 subsequently recruited by ARGONAUTE 4 (AGO4) (or other close paralog such as  
63 AGO6 and AGO9). The AGO4-siRNA complex associates with chromatin bound  
64 POLV-dependent transcripts produced from the same loci that will be methylated,  
65 through RNA-RNA pairing. The association between the AGO4-siRNA complex and  
66 POLV is further stabilized by protein-protein interactions between AGO4 and the  
67 CTD of POLV. Recruitment of the *de novo* DNA methyltransferase DOMAINS  
68 REARRANGED 2 (DRM2) to the template/target DNA occurs through the activity of  
69 RNA-DIRECTED DNA METHYLATION 1 (RDM1) that is able to bind methylated  
70 single stranded DNA (ssDNA) and also interacts with DRM2 and AGO4 (reviewed in  
71 Matzke & Moshier, 2014; Trujillo et al., 2018).

72 Retinoblastoma proteins are multi-faceted master regulators of cell reprogramming  
73 in eukaryotes and are involved in the control of cell cycle, DNA damage response  
74 and in protein-protein interactions (PPIs) with transcription factors that modulate  
75 stem cell maintenance and asymmetric cell division for proper cell lineage  
76 commitment (Calo et al., 2010; Cruz-Ramirez et al., 2012; Harashima & Sugimoto,  
77 2016; reviewed in Dyson, 2019; reviewed in Desvoyes & Gutiérrez, 2020). In  
78 Arabidopsis, RETINOBLASTOMA RELATED (RBR) has been shown to bind DNA,  
79 putatively to regulate the transcription of hundreds of genes and transposable  
80 elements (Bouyer et al., 2018) and also indirectly modulates gene expression by  
81 PPIs and genetic interactions with lineage-specific transcription factors (Cruz-  
82 Ramirez et al., 2012; Cruz-Ramirez et al., 2013; Matos et al., 2014; Zhao et al.,  
83 2017), chromatin-remodeling factors such as PICKLE (PKL) (Ötvös et al., 2021), and  
84 the Polycomb Repressor Complex 2 (PRC2) (Julien et al., 2018). The PRC2 complex  
85 regulates plant growth and development through the trimethylation of Lysine 27 on  
86 Histone 3 (H3K27me3), a well-known epigenetic mark involved in transcriptional  
87 repression. Two independent studies have established the connection between RBR  
88 and PRC2. Jullien *et al.*, (2008) demonstrated that RBR directly binds to

89 MULTICOPY SUPPRESSOR OF IRA1 (MSI1), an essential component of  
90 *Arabidopsis* PRC2 protein complexes involved in female gametogenesis, seed and  
91 vegetative development. The RBR-MSI1 complex directly represses *DNA*  
92 *METHYLTRANSFERASE 1 (MET1)* transcription, MET1 is a DNA methyltransferase  
93 acting on cytosine methylation at symmetrical CpG positions. *MET1* repression  
94 occurs only on the female gamete and is required for the expression of imprinted  
95 genes. A similar observation was also reported by Johnston *et al.* (2008). The  
96 interaction between RBR and PRC2 is potentially deeper since FERTILIZATION-  
97 INDEPENDENT ENDOSPERM (FIE), another member of the PRC2 complex that  
98 interacts with MEDEA (MEA), SWINGER (SWN) and CURLY LEAF (CLF) (Oliva *et*  
99 *al.*, 2016) does contain a highly conserved LxCxE motif, which is characteristic of  
100 proteins that bind with high-affinity to RBR (Cruz-Ramírez, *et al.*, 2012).

101 Plant and animal Retinoblastoma proteins share conserved residues that  
102 allow them to interact with proteins containing an LxCxE SLiM (SLiM: Short Linear  
103 Motif) RBR-binding motif (Lee *et al.*, 1998, Dick, 2007). A decade ago, a global  
104 search in the *Arabidopsis* proteome for proteins containing the LxCxE SLiM led us  
105 to the identification of hundreds of candidates that potentially interact with the single  
106 *Arabidopsis* Retinoblastoma protein: RBR. By employing the LxCxE motif, that  
107 confers high-affinity to RBR, as an *in silico* bait to identify *Arabidopsis* RBR protein  
108 partners (Cruz-Ramírez *et al.*, 2012), we identified several components of the RdDM  
109 pathway including the largest subunits of POLIV and POLV, RDR1, RDR2, DCL3,  
110 DRM2 and SUVR2 as potential targets of RBR. In this study we demonstrate that  
111 RBR binds to DRM2, DRD1 and SUVR2. We also report that seedlings of loss-of-  
112 function mutants in RBR and in genes of the RdDM pathway show phenotypes in  
113 the root apical meristem, with defects in the RSCN. This is consistent with the  
114 observation that RdDM and SUVR2 targets are up-regulated when RBR is post-  
115 transcriptionally silenced using the cell-type-specific artificial microRNA for Gene-  
116 silencing Overcome (amiGO) system. Our results uncover a novel mechanism for  
117 RBR function in transcriptional silencing through its interactions with key  
118 components of the RdDM pathway and opens the possibility of a convergent action  
119 of RBR-DRM2 in the regulation of TEs and lineage or tissue-specific transcription  
120 factors, and stem cell regulators, such as *WUSCHEL*, *AGL15* and *POLAR*, among  
121 other interesting putative target genes.

## 122 **Materials and Methods**

123

### 124 **Plant Materials**

125

126 *Arabidopsis thaliana* plants were grown as described in Cruz-Ramirez *et al.* (2004).  
127 Col-0 wild type, double (*nrpd2a-2;nrpd2b-1*) and triple mutants (*drm1;drm2;cmt3*)  
128 plants were used for phenotypic analyses, as well as transgenic lines  
129 (*pRBR::RBR:CFP*, *pDRM2::DRM2-GFP* and *35S::AmiGORBR*) (Cruz-Ramirez *et al.*  
130 *al.*, 2012; Cruz-Ramirez *et al.*, 2013).

131

### 132 **Microscopic Analysis**

133

134 Seedlings were grown and roots were prepared for confocal microscopy as  
135 previously described (Cruz-Ramirez *et al.*, 2012). Fluorescent signals for the diverse  
136 genetic backgrounds were recorded with a Leica SP2 CLSM and a Zeiss LSM 800  
137 CLSM. Roots were mounted and stained with Lugol as in Willemsen *et al.* (1998)  
138 and were visualized by Nomarski optics.

139

### 140 **Protein-Protein interaction (PPI) assays**

141

142 Yeast two-hybrid (Y2H) interactions were characterized by employing the ProQuest  
143 Two-Hybrid System (Invitrogen Life Technologies) as reported in Cruz-Ramirez *et al.*  
144 *al.*, (2013). To quantify the strength of each interaction, three biological and technical  
145 replicates of Beta-galactosidase assays with CPRG as substrate were performed.  
146 Bimolecular Fluorescence Complementation Assays in *Arabidopsis* protoplast were  
147 performed as reported in Cruz-Ramirez *et al.*, (2012). For RBR-DRM2, RBR-DRD1  
148 and controls YFP fluorescence was recorded with a Leica SP2 CLSM.

149

### 150 **Computational analyses and ortholog identification**

151 Angiosperm protein sequences were downloaded from Phytozome  
152 (<https://phytozome-next.jgi.doe.gov/>), while non-angiosperm and algae protein  
153 sequences were downloaded from Phytozome, Fernbase (Li *et al.*, 2018),  
154 TreeGenes (Wegrzyn *et al.*, 2019) and Phycocosm (Grigoriev *et al.*, 2021).  
155 Sequences for *A. agrestis* and *P. margaritaceum* were downloaded directly from the  
156 University of Zurich Hornworts database (Li *et al.*, 2020:  
157 <https://www.hornworts.uzh.ch/en.html>) and the Penium genome database (Jiao *et al.*,  
158 2020: <http://bioinfo.bti.cornell.edu/cgi-bin/Penium/blast.cgi>), respectively.  
159 LxCxE-SLiM containing protein sequences were detected using a custom perl script  
160 (Caballero-Perez, personal communication). To infer orthologues, all protein  
161 sequences from all 28 species analyzed were placed into orthogroups using the  
162 OrthoFinder software (Emms *et al.*, 2019).

163

164

## 165 **qRT-PCR assays of RdDM targets**

166 Twenty seedlings of 14-days-old post germination plants from Col-0 or  
167 *35S::AmiGORBR* (Cruz-Ramírez *et al.*, 2013), were used for total RNA extraction by  
168 TRIzol reagent (ThermoFisher) in three biological replicates. Total RNA was used to  
169 generate cDNAs according to the manufacturer's protocol for SuperScript III  
170 (ThermoFisher) we used 5 µg of total RNA per 20 µL reaction. The expression level  
171 was determined using SYBR GREEN mix (ThermoFisher) in a 10 µL reaction. The  
172 data were normalized using Actin 7 expression levels. The primers used in these  
173 experiments are those reported in Han *et al.* (2014).

174

## 175 **Results and discussion**

176

### 177 **Major players of the RdDM pathway and their putative RBR-Binding motifs**

178

179 Early predictions for Arabidopsis RBR-interactors, served as the basis for the  
180 functional characterization of the interaction between RBR with diverse lineage-  
181 specific factors such as SCARECROW, FAMA, XND1 and PICKLE, among others  
182 (Cruz-Ramírez *et al.*, 2012; Matos *et al.*, 2014; Zhao *et al.*, 2017; Zhou *et al.*, 2019;  
183 Ötvös, *et al.*, 2021). In addition to the aforementioned proteins, we identified many  
184 proteins with diverse key molecular and cellular functions bearing the RBR-binding  
185 motif which, in many cases, were evolutionarily conserved. Among them, we found  
186 that components of the RdDM pathway including NRPD2, DRD1, DRM2, DCL3 and  
187 SUVR2 contain the canonical LxCxE SLiM (Fig. 1, TableS1). We also found that  
188 major players of the RdDM pathway including NRPD1, NRPE and RDR2 contain a  
189 non-canonical RBR-interaction motif I/LxFxE (Fig. 1, TableS1). The observation that  
190 eight components of the RdDM pathway shared canonical and non-canonical RBR-  
191 interaction motifs prompted us to investigate if some of them are true physical RBR  
192 interactors.

193

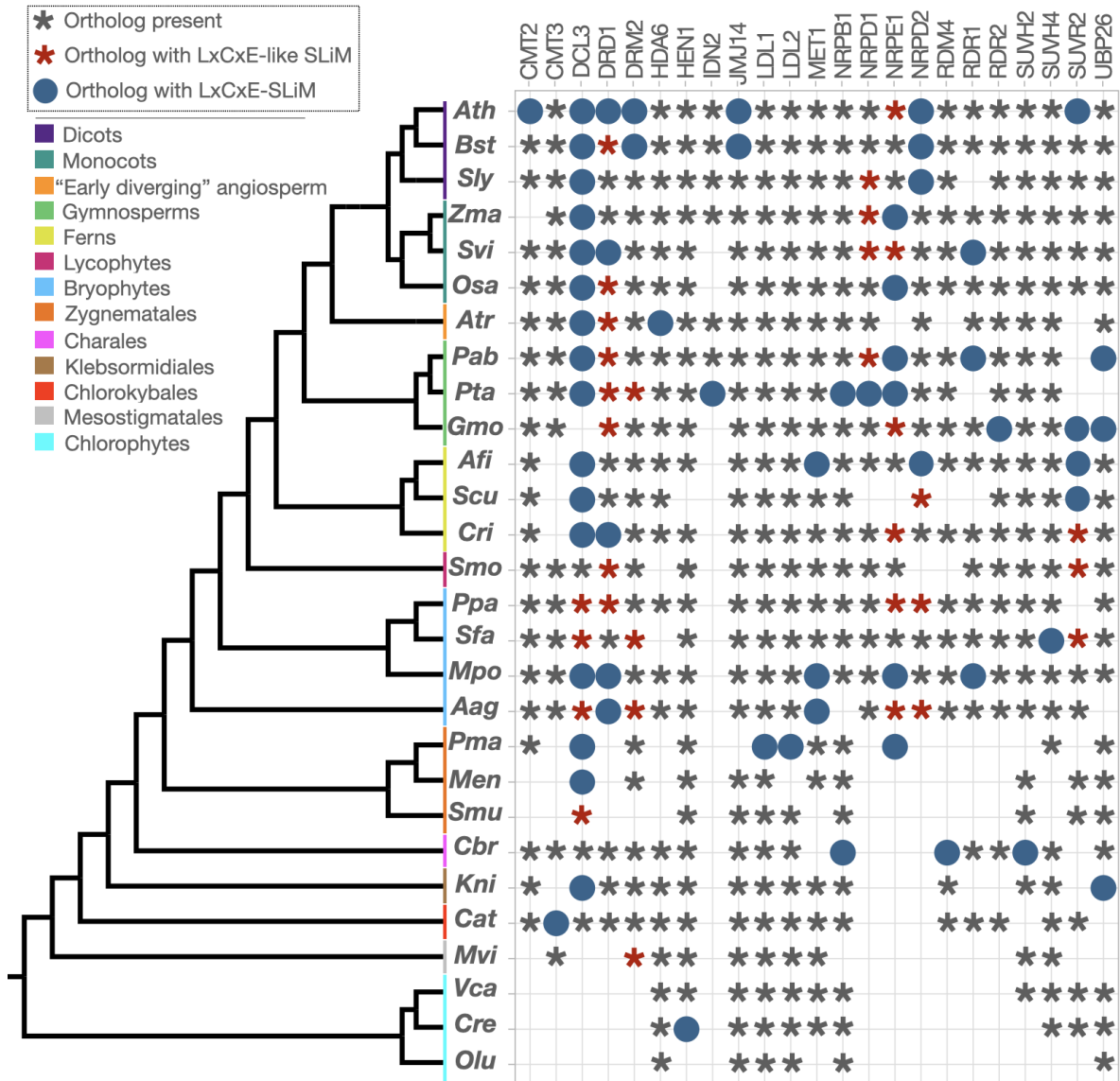
## 194 Conservation of LxCxE-like motifs in RdDM factors along Viridiplantae

195 To gain insight into the evolutionary conservation of the LxCxE SLiM present  
196 in components of the RdDM pathway, we interrogated publicly available plant and  
197 algae genomes aiming to detect the presence of canonical and non-canonical  
198 (LxCxE/LxCxD/LxCxD) LxCxE SLiMs among orthologs of the RdDM pathway along  
199 the Viridiplantae clade. To optimize the breadth of the plant phylogeny to cover, we  
200 focused on a small subset of species with available sequenced genomes  
201 representing each major lineage of the Viridiplantae kingdom. The species selected  
202 and analyzed include representatives from angiosperms (*A. thaliana* [Ath]; *Boechera*  
203 *stricta* [Bsf]; *Solanum lycopersicum* [Sly]; *Zea mays* [Zma]; *Setaria viridis* [Svi]; *Oryza*  
204 *sativa* [Osa]; *Amborella trichopoda* [Atr]), gymnosperms (*Picea abies* [Pab]; *Pinus*  
205 *taeda* [Pta]; *Gnetum montanum* [Gma]), ferns (*Azolla filliculoides* [Afi]; *Salvinia*  
206 *cucullata* [Scu]; *Ceratopteris richardii* [Cri]), lycophytes (*Selaginella moellendorffii*  
207 [Smo]), bryophytes (*Sphagnum fallax* [Sfa]; *Physcomitrium patens* [Ppa]; *Marchantia*  
208 *polymorpha* [Mpo]; *Anthoceros agrestis* [Aag]) charophyte (*Penium margaritaceum*  
209 [Pma]; *Mesotaenium endlicheranium* [Men]; *Spirogloea muscicola* [Smu]; *Chara*  
210 *braunii* [Cbr]; *Klebsormidium nitens* [Kni]; *Chlorokybus atmophyticus* [Cat];  
211 *Mesostigma viride* [Mvi]) and chlorophyte (*Volvox carteri* [Vca]; *Chlamydomonas*  
212 *reinhardtii* [Cre]; *Ostreococcus lucimarinus* [Olu]) algae.

213 Our analysis revealed that *A. thaliana* was the species with more proteins  
214 containing either canonical or non-canonical RBR-binding motifs (Fig. 1, Table S1),  
215 with 8 out of 23 RdDM-related proteins analysed (DCL3, DRD1, DRM2, NRPD2,  
216 SUVR2, CMT2, JMJ14 and NRPE1). DCL3 orthologs showed the highest level of  
217 conservation for canonical and non-canonical LxCxE SLiMs among the species  
218 analyzed as they are absolutely conserved in tracheophytes, with the only exception  
219 of *G. montanum*. Interestingly, while DCL3 in *M. polymorpha* bears a canonical  
220 LxCxE SLiM, DCL3 orthologs in other bryophytes specifically *S. fallax*, *P. patens* and  
221 *A. agrestis* contain LxCxE-like SLiMs. From the seven charophyte algae species  
222 analysed, 3 of them contain canonical RBR-binding motif (*P. margaritaceum*,  
223 *M. endlicheranium*, *K nitens*) while *S. muscicola* contains an LxCxE SLiM (Fig. 1, Table  
224 S1). Although the LxCxE SLiM is highly conserved along DCL3 orthologs, it is difficult  
225 to determine if the canonical or the non-canonical motif is the ancestral one.

226 DRD1 orthologues showed the presence of the LxCxE SLiM in a patchy  
227 pattern along the plant lineages analyzed. The presence of the LxCxE SLiM in DRD1  
228 orthologues is less conserved than in DCL3 orthologues since we were not able to  
229 find LxCxE or LxCxE-like SLiMs in any of the algae species analyzed, however it is  
230 present in *Marchantia*, *Anthoceros*, and *Ceratopteris* DRD1 orthologs (Fig. 1,  
231 TableS1). The presence of the LxCxE SLiM is even less conserved in DRM2  
232 orthologs than in DRD1, with only two DRM2 orthologs from *Arabidopsis* and  
233 *Boechera* exhibiting a canonical SLiM and non-canonical LxCxE SLiMs present in

234 *Pinus*, *Sphagnum*, *Antoceros* and *Mesostigma*. In the case of the subunits of POLIV  
235 and POLV, we expanded a presence-absence analysis along the plant phylogeny,  
236 similar to that reported previously by Huang *et al.* (2015). We found that NRPE1,  
237 NRPD1 and NRPD2 showed the presence of both canonical and non-canonical  
238 LxCxE SLiMs in diverse species, among these 3 proteins we found that NRPE1 is  
239 the one with more species containing either canonical or non-canonical RBR-binding  
240 SLiM (Fig. 1, TableS1). While Arabidopsis NRPD1 does not contain an LxCxE SLiM,  
241 *P. taeda* NRPD1 ortholog contains a canonical LxCxE SLiM and orthologs from *S.*  
242 *viridis*, *P. abies*, maize and tomato bear a non-canonical LxCxE SLiM. We observed  
243 the presence of canonical LxCxE SLiMs in NRPE1 from charophyte to flowering  
244 plants (*P. margaritaceum*, *M. polymorpha*, *P. abies*, *P. taeda*, *Z. mays* and *O. sativa*)  
245 and non-canonical LxCxE SLiMs in NRPE1 orthologs from *C. richardii*, *A. agrestis*,  
246 *P. patens*, *G. montanum*, *S. viridis* and *A. thaliana*. The presence of canonical and  
247 noncanonical LxCxE SLiMs involved in RBR-binding in the POLIV and POLV largest  
248 subunits (NRPD1 and NRPE1, respectively) and the shared second largest subunit  
249 (NRPD/E2) strongly suggests that a new layer of regulation of the RdDM pathway  
250 mediated by RBR is present in land plants.



251

252 **Fig. 1.** Phylogenetic conservation of canonical (solid blue circle) and non-canonical (red  
 253 asterisk) LxCxE SLiMs in orthologs of the RdDM pathway in representative species along  
 254 Viridiplantae.

255

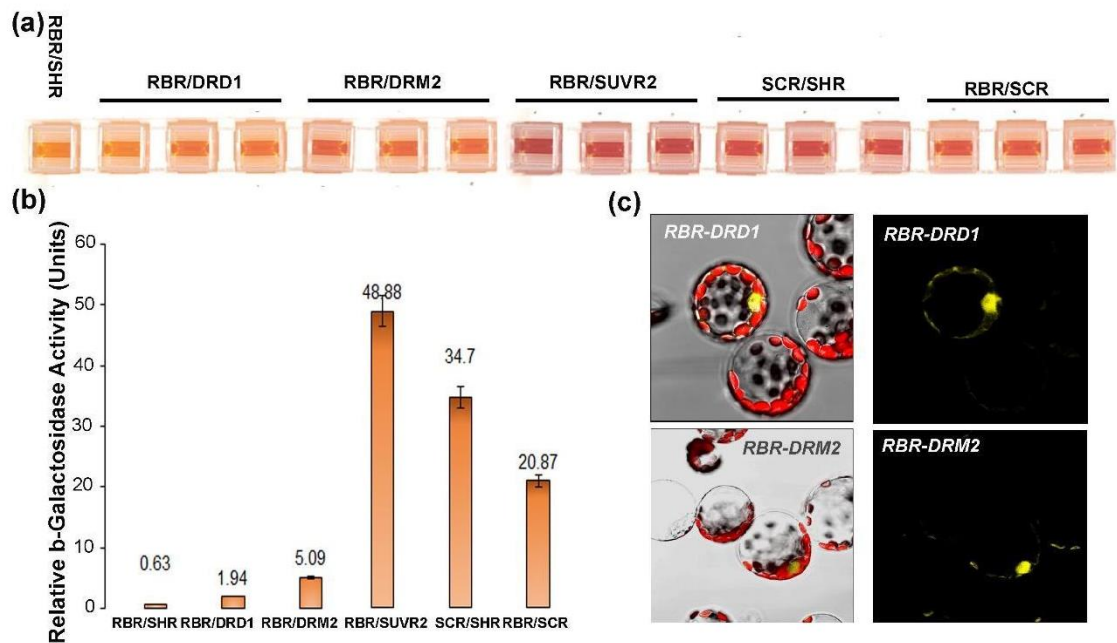
## 256 **DRM2, DRD1 and SUVR2 physically interact with RBR**

257 Based on their conservation patterns we selected a group of proteins to test  
 258 for protein-protein interactions with RBR. We generated constructs using amplified  
 259 coding sequences (CDS) of DRM2, DRD1 and SUVR2 from *Arabidopsis* for Y2H  
 260 assays, in order to test if they interact with RBR (previously cloned in pDEST32 and  
 261 used in Cruz-Ramirez *et al.*, 2012). Our results showed that SUVR2 strongly  
 262 interacts with RBR when quantified and compared with other partners and controls  
 263 (Fig.2 a, b) but DRD1 and DRM2 showed weak interaction. The previously described



264 Y2H results prompted us to confirm, using a semi *in vivo* system, DRD1-RBR and  
265 DRM2-RBR interactions by Bimolecular Fluorescence Complementation (BiFC)  
266 assays. We found that YFP nuclear signal is clear and evident in *Arabidopsis*  
267 mesophyll protoplasts, confirming that DRD1 and DRM2 do interact with RBR. We  
268 also found that the *M. polymorpha* DCL3 ortholog interacts with both *Arabidopsis*  
269 and *M. polymorpha* RBRs by Y2H assays (León-Ruiz & Cruz-Ramirez, *in*  
270 *preparation*). Further experimental work is required to confirm PPIs between RBR  
271 and other RdDM-related proteins including NRPD1, NRPE1 and NRPD/E2 but it is  
272 important to consider that regulation by RBR can go beyond its direct interactors, for  
273 example it can affect other PPIs indirectly as documented in the IntAct Molecular  
274 Interactions Database from EMBL-EBI: DRM2 establishes 12 PPIs, from which at  
275 least 4 are direct interactions with members of the RdDM pathway, such as RDM1,  
276 AGO4, AGO9, and ZOP1 (Fig.4d.  
277 (<https://www.ebi.ac.uk/intact/interactions?conversationContext=4>). Taken together,  
278 our results indicate that the evolutionary conservation of LxCxE SLiMs among  
279 components of the RdDM pathway is consistent with our experimentally validated  
280 interactions with RBR in the cases of DRD1, DRM2 and SUVR2.

281



282

283 **Fig. 2.** (a) Yeast two-hybrid analyses showing  $\beta$ -gal colorimetric reaction and its quantitation,  
284 in (b), for diverse proteins of the RdDM pathway and RBR. SCR-RBR and SCR-SHR  
285 combinations are positive controls, and RBR-SHR is the negative control (Cruz-Ramírez,  
286 et al, 2013) (c) RBR-DRD1 and RBR-DRM2 binding by BiFC in *Arabidopsis* mesophyll  
287 protoplasts.

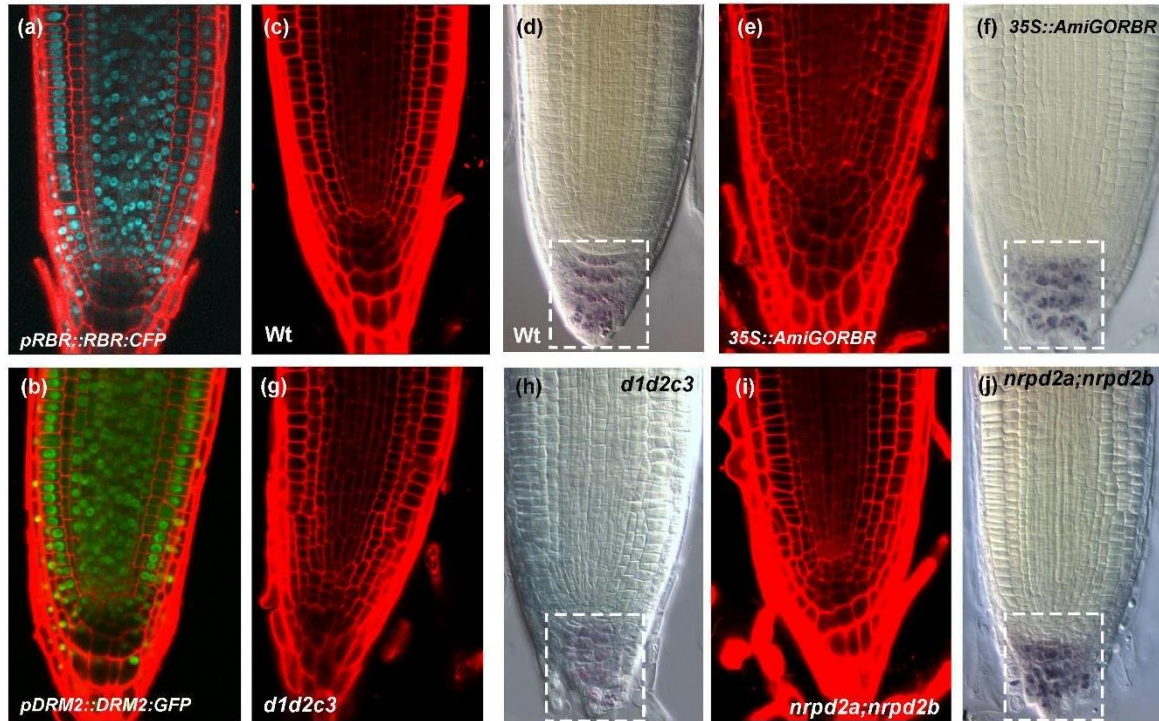
288

289 **RdDM and RBR loss-of-function mutants show similar developmental**  
290 **alterations**

291 It has been shown that loss of function mutants in members of the RdDM pathway  
292 show phenotypes in diverse developmental processes and stages of *Arabidopsis*  
293 (He *et al.*, 2009; reviewed in Matzke *et al.*, 2015; Mendes *et al.*, 2020).

294 In addition to physically interacting, RBR and DRM2 protein fusions  
295 (pRBR::RBR:CFP, pDRM2::DRM2:GFP) have quite similar expression patterns as  
296 both proteins are present in every cell of the RAM (Fig.3 a,b). Since RBR has been  
297 shown to regulate stem cells and QC divisions in the Arabidopsis RAM (Cruz-  
298 Ramirez *et al.*, 2012; Cruz-Ramirez, *et al.*, 2013), we wondered if loss of function  
299 (LOF) mutants, in tested and putative interactors, in genes of the RdDM pathways  
300 may display similar phenotypes to those in RBR LOF lines. Therefore, we analyzed  
301 root development of 12 dpg (days post germination) seedlings of the  
302 *drm1;drm2;cmt3* triple mutant and the *nrpd2a;nrpd2b* double mutant and observed  
303 that primary root development in these mutants is affected. Although the phenotype  
304 is variable among seedlings from mild to severe, they all exhibit a shorter  
305 meristematic zone (Fig.S1 a, b, c). We analyzed in detail the organization of the RAM  
306 and root stem cell niche (RSCN) of *drm1;drm2;cmt3* and *nrpd2a;nrpd2b* 10 dpg  
307 seedlings and observed that roots from both mutant lines showed a disorganized  
308 RAM and defects in the columella region relative to wild-type seedlings (Fig.3). In  
309 addition, the loss of function in RBR causes QC divisions, extra stem cells and  
310 aberrant divisions and alterations in the columella region, as revealed for the  
311 analysis of the *35S::AmiGO-RBR* RAM (Fig.3 e, f). Columella phenotypes observed  
312 in RdDM and RBR loss-of-function mutants, shown in Fig.3 and Fig.S1, are  
313 consistent with findings in this tissue by Kawakatsu *et al.* (2016), who reported that  
314 the *Arabidopsis* columella root cap genome is hypermethylated and transcripts  
315 encoding RdDM factors, as well as 24-nt small RNAs (smRNAs), are more abundant  
316 in this tissue than any other root cell type.

317



318

319 **Fig. 3.** Longitudinal root sections of 10 dpg seedlings imaged by confocal laser scanning  
320 microscope (CLSM) (a), (b), (c), (e), (g), (i), and Nomarski optics of lugol-stained roots (d),  
321 (f), (h) and (j). Panels (a) and (b) show the expression patterns of *pRBR::RBR:CFP* and  
322 *pDRM2::DRM2:GFP*. (c) confocal and (d) Nomarski optics images showing root apical  
323 meristem (RAM) and root stem cell niche (RSCN) organization in Col-0 (WT) seedlings. (e)  
324 Confocal and (f) Nomarski images of *35S::AmiGO-RBR* seedlings showing alterations in the  
325 RAM and RSCN. (g) Confocal and (h) Nomarski images of *drm1;drm2;cmt3* (*d1d2c3*) triple  
326 mutant seedlings showing alterations in the RAM and the RSCN. (i) Confocal and (j)  
327 Nomarski images of *nrpd2a;nrpd2b* double mutant seedlings showing phenotypes in the  
328 RAM and RSCN, dotted squares highlight the Columella region.

329

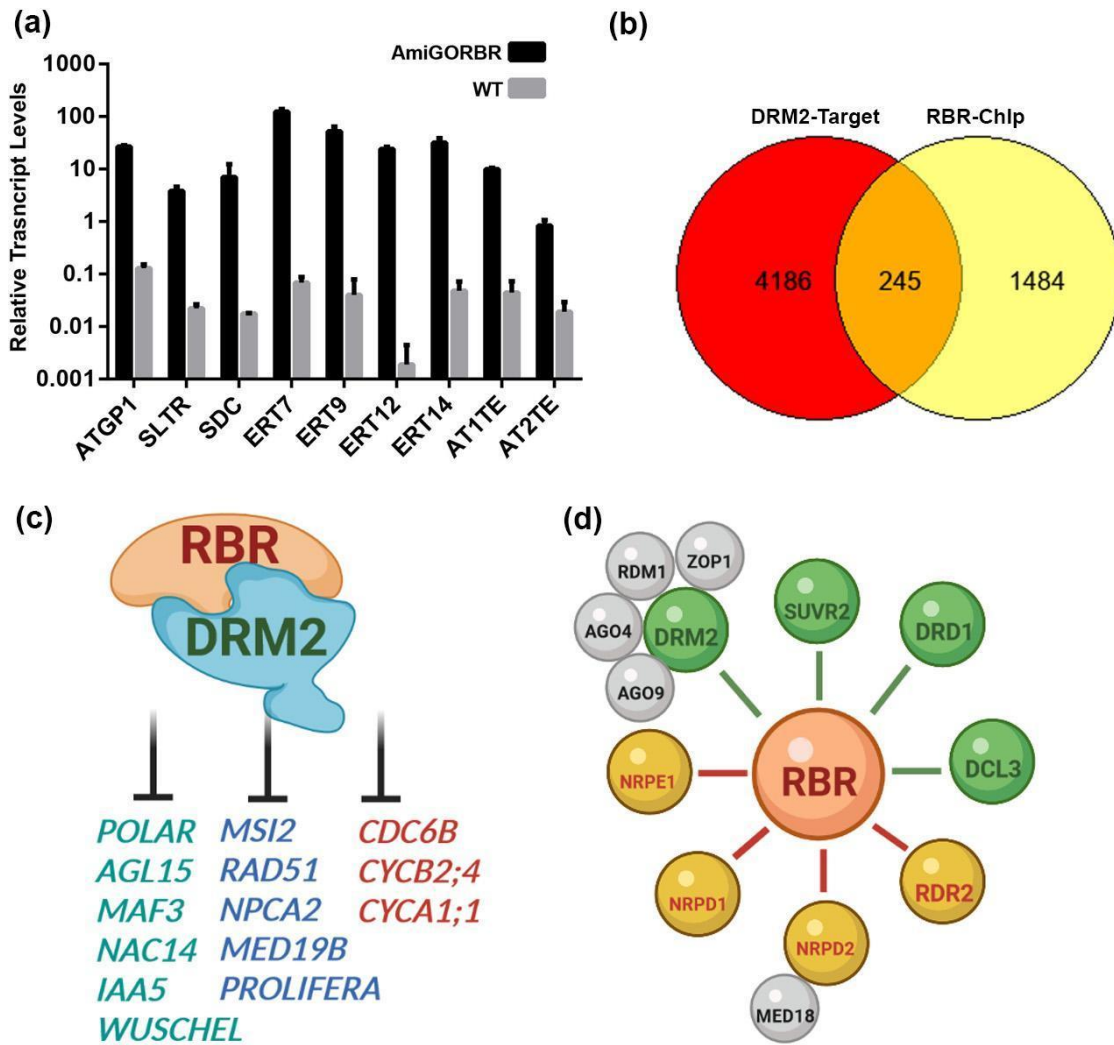
### 330 **RdDM and SUVR2 targets are up-regulated in the AmiGO-RBR background**

331 SUVR2 silences a subset of RdDM target loci, as well as RdDM-independent targets  
332 (Hang *et al.*, 2014). Well-known targets of RdDM include TEs from the solo LTR  
333 (SLTR) and AtGP1 LTR families and genes such as *SUPPRESSOR OF drm1 drm2*  
334 *cmt3* (*SDC*) and it has been shown that at *SDC* and *ERT7* loci, the *suvr2* loss-of-  
335 function mutants display a synergistic phenotype with mutants in key genes of the  
336 RdDM pathway, which suggests that at these loci SUVR2 might exert silencing  
337 through a pathway which is partially independent of RdDM (Hang *et al.*, 2014). Our  
338 data indicates that SUVR2, DRM2 and DRD1 bind *in vitro* to RBR and based on the  
339 presence of the LxCxE SLiM other RdDM components like NRPD1, NRPE1 and  
340 DCL3 could also potentially bind to RBR. Therefore, we wondered if the silencing of  
341 several RdDM and SUVR2 target loci may be affected in a *35S::AmiGO-RBR*

342 background. To answer such question, we isolated total RNA of 12-days-old wild-  
343 type and *35S::AmiGO-RBR* seedlings and performed qRT-PCR assays using  
344 previously-reported primers for *SDC*, *AtGP1*, *solo LTR* (SLTR), AT1TE51360  
345 (AT1TE), AT2TE78930 (AT2TE), ERT7, ERT9, ERT12, and ERT14. Our results  
346 showed that all tested loci are either moderately or strongly up-regulated in the RBR  
347 loss-of-function background relative to the wild-type control (Fig.4a). It has been  
348 shown that *ERT9* transcripts are not de-repressed in the *suvr2* mutant background,  
349 suggesting that RBR might influence DRM2 and SUVR2 targets independently.  
350 Overall, these results indicate that RBR acts repressing RdDM and SUVR2  
351 transposable elements targets. Whether this action depends on RBR protein-protein  
352 interaction with DRM2, SUVR2 or DRD1 remains to be answered in future studies.

353 The RdDM pathway methylates not only TE loci, but also hundreds of protein-  
354 coding genes (Jha & Shanka, 2014). Since RBR also has hundreds of targets,  
355 predicted by Chip-Seq (Bouyer *et al.*, 2018), we explored a potential overlap  
356 between the 4,431 DRM2 methylation targets proposed by Jha and Shankar (2014)  
357 and the 1,729 RBR target genes predicted by Bouyer *et al.*, (2018). We found that  
358 245 target genes are shared between RBR and DRM2 (Fig.4b). Among the 245  
359 shared target genes we found several interesting ones (Fig. 4c). We highlighted  
360 those that encode transcriptional regulators such as *POLAR LOCALIZATION*  
361 *DURING ASYMMETRIC DIVISION AND REDISTRIBUTION (POLAR)*, *AGAMOUS*  
362 *LIKE 15*, *NAC15*, *INDOLE-3-ACETIC ACID INDUCIBLE 5 (IAA5)* and *MADS*  
363 *AFFECTING FLOWERING 3 (MAF3)*. Another important transcription factor that has  
364 been shown to act downstream RBR is *WUSCHEL*. In *rbr1-2* mutants,  
365 supernumerary megaspore mother cells (MMCs) are formed, a phenotype that  
366 correlates with *WUS* transcriptional deregulation Zhao *et al.* (2017). Indeed these  
367 authors demonstrate that RBR binds to a specific region on the *WUS* promoter. It  
368 has also been shown that in the *drm1;drm2;cmt3* *WUS* transcription is de-repressed  
369 during root regeneration and that two non-CG sites in the promoter of this gene might  
370 be related to *WUS* silencing in *Arabidopsis* roots (Shermer *et al.*, 2015). Recently  
371 Mendes *et al.* (2020) showed that *drm1;drm2* double mutants develop multiple  
372 MMCs, a phenotype also described for other mutants in key genes of the RdDM  
373 pathway, such as *rdr6* and *ago9* (Olmedo-Monfil *et al.*, 2010). We also found that  
374 genes related to DNA integrity, DNA replication and cell cycle are common targets  
375 of RBR and DRM2, such as *RAD51*, *PROLIFERATING CELL NUCLEAR ANTIGEN*  
376 *2 (PCNA2)*, *MINICHROMOSOME MAINTENANCE 7/PROLIFERA (MCM7)*, *MS1*,  
377 *MEDIATOR 19B (MED19B)*, *CYCLIN A1;1 (CYCA1;1)*, *CELL DIVISION CONTROL*  
378 *6B (CDC6B)* and *CYCLIN B2;4 (CYCB2;4)* (Table S2). The putative function of RBR  
379 and DRM2 acting on the silencing of genes involved in cell cycle progression, which  
380 are normally expressed only in root meristematic cells, such as *CDC6B* or *CYCA1;1*,  
381 correlate with some of the root phenotypes reported in Fig. 3 and Fig.S1. However,  
382 root phenotypes in RdDM mutants are not similar in all cases, and such contrasting  
383 phenotypes may be caused by the deregulation of hundreds of genes with diverse  
384 cellular functions.

385 Overall, this study uncovers novel mechanisms for RBR function in transcriptional  
386 silencing through interacting with components of the RdDM pathway and opens  
387 novel working hypotheses for diverse potential RBR-RdDM interactions (Fig. 4d),  
388 including the RBR-DRM2 complex, regulating TEs and interesting lineage-specific  
389 transcription factors.



390

391 **Fig. 4.** (a) Transcript levels revealed by qRT-PCR of RdDM targets in the AmiGO-RBR  
 392 mutant background vs the control, (b) RBR-ChIP and DRM2-mediated DNA methylation  
 393 common targets, (c) Key examples of RBR-DRM2 common targets, (d) RdDM proteins that  
 394 have been validated as RBR direct interactors (green lines) and those that are putatively  
 395 binding RBR (red lines), gray balloons are PPIs with DRM2 reported in the IntAct database  
 396 <https://www.ebi.ac.uk/intact/interactions?conversationContext=4>, (Created with  
 397 [BioRender.com](https://www.biorender.com)).

398

399

400

401

402 **Acknowledgements**

403 We wish to thank Vicki Chandler, Steve Jacobsen, Fred Berger and Pauline Jullien  
404 for sharing published plant materials. We also thank Dr. Juan Caballero-Pérez for  
405 initial advice on bioinformatics. J L-R (CVU 858608) was supported by Consejo  
406 Nacional de Ciencia y Tecnología (CONACYT) with a PhD Fellowship. A C-R was  
407 supported by EMBO-ALTF 1114-2006 and CONACYT 000000000092916 grants. M  
408 A-V was supported by Consejo Nacional de Ciencia y Tecnología (CONACYT)  
409 grants 158550 and A1-S-38383 and Newton Fund of the Royal Society grant  
410 NA150181.

411

412 **Author contributions**

413 Conceived the project: A C-R and M A-V. Performed *wetlab* and *in silico*  
414 experiments: A C-R, A E-C, J L-R, I B. Analyzed the data: A C-R, M A-V, B S, I B, A  
415 E-C and J L-R. Contributed reagents and equipment: B S, M A-V, A C-R. Wrote the  
416 manuscript with inputs from all coauthors: AC-R and MA-V.

417 **ORCID**

418 A C-R <https://orcid.org/0000-0001-9973-5784>

419 M A-V <https://orcid.org/0000-0002-9435-0049>

420 B S <https://orcid.org/0000-0001-5400-9578>

421 I B <https://orcid.org/0000-0001-8003-3782>

422 A E-C <https://orcid.org/0000-0002-5421-1503>

423

424

425

426

427 **References**

- 428 Ausin I, Greenberg MV, Simanshu DK, Hale CJ, Vashisht AA, Simon SA, Lee TF,  
429 Feng S, et al. 2012 . INVOLVED IN DENOVO 2-containing complex involved in  
430 RNA-directed DNA methylation in Arabidopsis. *Proc. Natl. Acad. Sci. USA* 109  
431 8374–8381.
- 432 Borges F, Martienssen RA. 2015. The expanding world of small RNAs in plants.  
433 *Nat Rev Mol Cell Biol.* 16(12):727-41.
- 434 Bouyer D, Heese M, Chen P, Harashima H, Roudier F, Grüttner C, Schnittger A.  
435 2018. Genome-wide identification of RETINOBLASTOMA RELATED 1 binding sites  
436 in Arabidopsis reveals novel DNA damage regulators. *PLoS Genet.*  
437 14(11):e1007797.
- 438  
439 Calo E, Quintero-Estades JA, Danielian PS, Nedelcu S, Berman SD, Lees JA. 2010.  
440 Rb regulates fate choice and lineage commitment in vivo. *Nature.*  
441 26;466(7310):1110-1114.
- 442  
443 Cruz-Ramírez A, López-Bucio J, Ramírez-Pimentel G, Zurita-Silva A, Sánchez-  
444 Calderon L, Ramírez-Chávez E, González-Ortega E, Herrera-Estrella L. 2004. The  
445 xipotl mutant of Arabidopsis reveals a critical role for phospholipid metabolism in root  
446 system development and epidermal cell integrity. *Plant Cell.* 2004 16(8):2020-2034.
- 447 Cruz-Ramírez A, Díaz-Triviño S, Blilou I, Grieneisen VA, Sozzani R, Zamioudis C,  
448 Miskolczi P, Nieuwland J, Benjamins R, Dhonukshe P, Caballero-Pérez J, Horvath  
449 B, Long Y, Mähönen AP, Zhang H, Xu J, Murray JA, Benfey PN, Bako L, Marée AF,  
450 Scheres B. 2012. A bistable circuit involving SCARECROW-RETINOBLASTOMA  
451 integrates cues to inform asymmetric stem cell division. *Cell.* 31;150(5):1002-1015.
- 452 Erdmann RM, Picard CL. 2020. RNA-directed DNA Methylation. *PLoS Genet.*  
453 16(10):e1009034.
- 454 Haag JR, Pikaard CS. 2011. Multisubunit RNA polymerases IV and V: purveyors of  
455 non-coding RNA for plant gene silencing. *Nat Rev Mol Cell Biol.* 12(8):483-92.
- 456 Han YF, Dou K, Ma ZY, Zhang SW, Huang HW, Li L, Cai T, Chen S, Zhu JK, He XJ.  
457 2014. SUVR2 is involved in transcriptional gene silencing by associating with SNF2-  
458 related chromatin-remodeling proteins in Arabidopsis. *Cell Res.* 24(12):1445-1465.
- 459 He XJ, Hsu YF, Zhu S, Liu HL, Pontes O, Zhu J, Cui X, Wang CS, Zhu JK. 2009. A  
460 conserved transcriptional regulator is required for RNA-directed DNA methylation  
461 and plant development. *Genes Dev.* 1;23(23):2717-22.
- 462 Huang Y, Kendall T, Forsythe ES, Dorantes-Acosta A, Li S, Caballero-Pérez J, Chen  
463 X, Arteaga-Vázquez M, Beilstein MA, Mosher RA. 2015. Ancient Origin and Recent  
464 Innovations of RNA Polymerase IV and V. *Mol Biol Evol.* 32(7):1788-1799.



- 465 Jha A, Shankar R. 2014. MiRNAting control of DNA methylation. *J Biosci.* 39(3):365-  
466 380.
- 467 Johnston AJ, Matveeva E, Kirioukhova O, Grossniklaus U, Grissem W. 2008. A  
468 dynamic reciprocal RBR-PRC2 regulatory circuit controls Arabidopsis gametophyte  
469 development. *Curr Biol.* 18(21):1680-1686.
- 470 Jullien PE, Mosquna A, Ingouff M, Sakata T, Ohad N, Berger F. 2008.  
471 Retinoblastoma and its binding partner MSI1 control imprinting in Arabidopsis. *PLoS*  
472 *Biol.* 12;6(8):e194.
- 473 Jullien PE, Susaki D, Yelagandula R, Higashiyama T, Berger F. 2012. DNA  
474 methylation dynamics during sexual reproduction in Arabidopsis thaliana. *Curr Biol.*  
475 9;22(19):1825-1830.
- 476 Kawakatsu T, Stuart T, Valdes M, Breakfield N, Schmitz RJ, Nery JR, Urich MA, Han  
477 X, Lister R, Benfey PN, Ecker JR. 2016. Unique cell-type-specific patterns of DNA  
478 methylation in the root meristem. *Nat Plants.* 29;2(5):16058.
- 479 Law JA, Jacobsen SE. 2010. Establishing, maintaining and modifying DNA  
480 methylation patterns in plants and animals. *Nat Rev Genet.* 11(3):204-20.
- 481 Matos JL, Lau OS, Hachez C, Cruz-Ramírez A, Scheres B, Bergmann DC. 2014.  
482 Irreversible fate commitment in the Arabidopsis stomatal lineage requires a FAMA  
483 and RETINOBLASTOMA-RELATED module. *Elife.* 10;3:e03271.
- 484 Matzke MA, Mosher RA. 2014. RNA-directed DNA methylation: an epigenetic  
485 pathway of increasing complexity. *Nat Rev Genet.* 15(6):394-408.
- 486 Matzke MA, Kanno T, Matzke AJ. RNA-Directed DNA Methylation: The Evolution of  
487 a Complex Epigenetic Pathway in Flowering Plants. 2015. *Annu Rev Plant Biol.*  
488 2015;66:243-67.
- 489 Mendes MA, Petrella R, Cucinotta M, Vignati E, Gatti S, Pinto SC, Bird DC, Gregis  
490 V, Dickinson H, Tucker MR, Colombo L. 2020. The RNA-dependent DNA  
491 methylation pathway is required to restrict SPOROCTELESS/NOZZLE expression  
492 to specify a single female germ cell precursor in Arabidopsis. *Development.*  
493 147(23):dev194274.
- 494 Oliva M, Butenko Y, Hsieh TF, Hakim O, Katz A, Smorodinsky NI, Michaeli D, Fischer  
495 RL, Ohad N. 2016. FIE, a nuclear PRC2 protein, forms cytoplasmic complexes in  
496 Arabidopsis thaliana. *J Exp Bot.* 67(21):6111-6123.
- 497 Olmedo-Monfil V, Durán-Figueroa N, Arteaga-Vázquez M, Demesa-Arévalo E,  
498 Autran D, Grimanelli D, Slotkin RK, Martienssen RA, Vielle-Calzada JP. 2010.  
499 Control of female gamete formation by a small RNA pathway in Arabidopsis. *Nature.*  
500 464(7288):628-32.

501 Ötvös K, Miskolczi P, Marhavý P, Cruz-Ramírez A, Benková E, Robert S, Bakó L.  
502 2021. Pickle Recruits Retinoblastoma Related 1 to Control Lateral Root Formation  
503 in Arabidopsis. *Int J Mol Sci.* 8;22(8):3862.

504 Shemer O, Landau U, Candela H, Zemach A, Eshed Williams L. 2015. Competency  
505 for shoot regeneration from Arabidopsis root explants is regulated by DNA  
506 methylation. *Plant Sci.* 238:251-261.

507 Trujillo JT, Seetharam AS, Hufford MB, Beilstein MA, Mosher RA. 2018. Evidence  
508 for a Unique DNA-Dependent RNA Polymerase in Cereal Crops. *Mol Biol Evol.*  
509 35(10):2454-2462.

510 Willemsen V, Wolkenfelt H, de Vrieze G, Weisbeek P, Scheres B. 1998. The  
511 HOBBIT gene is required for formation of the root meristem in the Arabidopsis  
512 embryo. *Development.* 125(3):521-531.

513  
514 Zhang Y, Shi C, Fu W, Gu X, Qi Z, Xu W, Xia G. Arabidopsis MED18 Interaction  
515 With RNA Pol IV and V Subunit NRPD2a in Transcriptional Regulation of Plant  
516 Immune Responses. 2021. *Front Plant Sci.* 6;12:692036.

517  
518 Zhao C, Lasses T, Bako L, Kong D, Zhao B, Chanda B, Bombarely A, Cruz-Ramírez  
519 A, Scheres B, Brunner AM, Beers EP. 2017. XYLEMNAC DOMAIN1, an angiosperm  
520 NAC transcription factor, inhibits xylem differentiation through conserved motifs that  
521 interact with RETINOBLASTOMA-RELATED. *New Phytol.* 216(1):76-89.

522  
523 Zhao X, Bramsiepe J, Van Durme M, Komaki S, Prusicki MA, Maruyama D, Forner  
524 J, Medzihradzsky A, Wijnker E, Harashima H, Lu Y, Schmidt A, Guthörl D, Logroño  
525 RS, Guan Y, Pochon G, Grossniklaus U, Laux T, Higashiyama T, Lohmann JU,  
526 Nowack MK, Schnittger A. 2017. RETINOBLASTOMA RELATED1 mediates  
527 germline entry in Arabidopsis. *Science.* 28;356(6336):eaaf6532.

528  
529 Zhou W, Lozano-Torres JL, Blilou I, Zhang X, Zhai Q, Smant G, Li C, Scheres B.  
530 2019. A Jasmonate Signaling Network Activates Root Stem Cells and Promotes  
531 Regeneration. *Cell.* 177(4):942-956e.

532

533

534

535

536

537

538

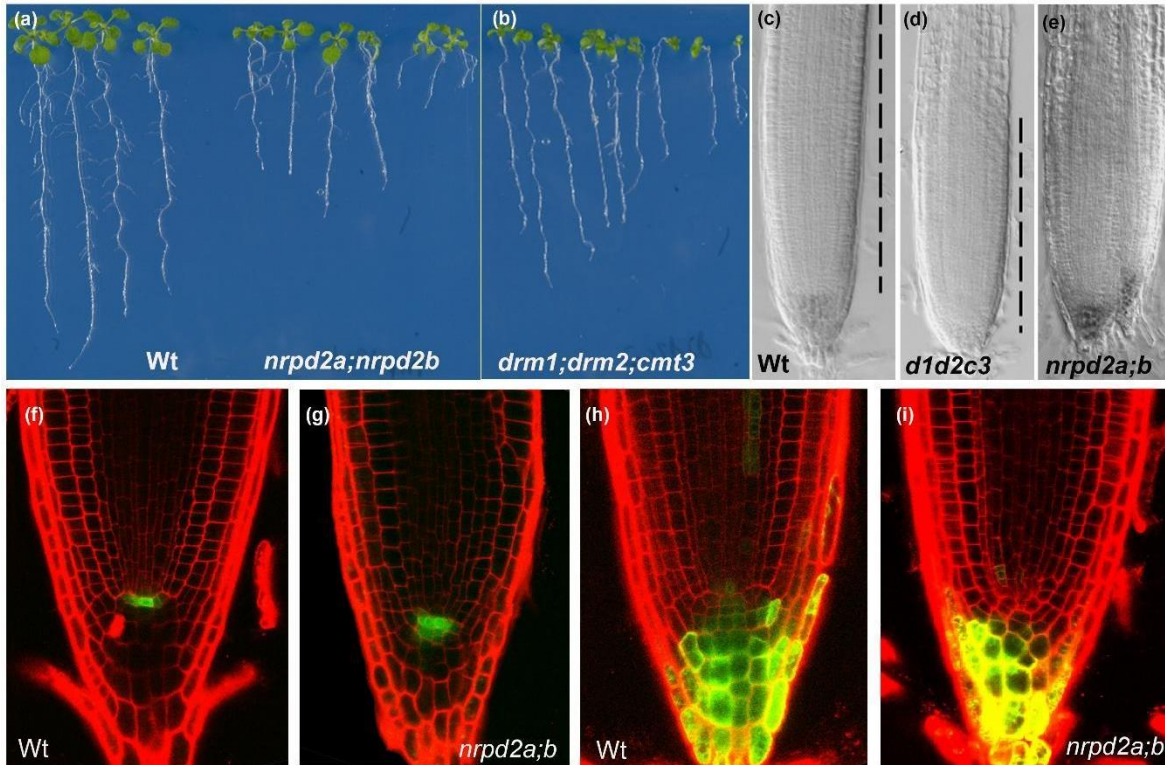
539

540 **Supporting information**

541

542 **Fig.S1.** RAM phenotypes in RdDM mutants.

543



544

545 **Fig. S1.** Root and shoot phenotypes, recorded with stereomicroscope, of 10 days post  
546 germination (dpg) seedlings of wild-type (a), double and triple mutants in RdDM proteins (a),  
547 (b). Nomarski optics for RAM phenotypes of *drm1;drm2;cmt3* and *nrpd2a;nrpd2b* mutant (d),  
548 (e) and wild-type (c) roots of 10 dpg seedlings. Longitudinal root sections of 10 dpg seedlings  
549 by confocal laser scanning microscope (CLSM) of *pWOX5::GFP* and *TCS::GFP* transgenes  
550 in WT (f), (h) and *nrpd2a;nrpd2b* (g), (i) backgrounds, respectively.